

# Rare decays $B \rightarrow X_s \tau^+ \tau^-$ and $B_s \rightarrow \tau^+ \tau^- \gamma$ in technicolor with scalars

Zhaohua Xiong <sup>a,b,c</sup> and Jin Min Yang <sup>b</sup>

<sup>a</sup> CCAST (World Laboratory), P.O.Box 8730, Beijing 100080, China

<sup>b</sup> Institute of Theoretical Physics, Academia Sinica, Beijing 100080, China

<sup>c</sup> Institute of High Energy Physics, Academia Sinica, Beijing 100039, China

(November 6, 2018)

We examine the rare decays  $B \rightarrow X_s \tau^+ \tau^-$  and  $B_s \rightarrow \tau^+ \tau^- \gamma$  in the framework of technicolor with scalars. The contributions from both the neutral and charged scalars predicted in this model are evaluated. We find that the branching ratios could be enhanced over the standard model predictions by a couple of orders of magnitude in some part of parameter space. The forward-backward asymmetry and the distributions of differential branching ratios are also found to differ significantly from the standard model results. Such large new physics effects might be observable in the new generation of B experiments.

12.60.NZ, 13.25.Hw

**Key words:** Technicolor with scalars; Decay  $B \rightarrow X_s \tau^+ \tau^-$ ; Decay  $B_s \rightarrow \tau^+ \tau^- \gamma$ ; Forward-backward asymmetry

## I. INTRODUCTION

One intriguing puzzle in particle physics is the regular pattern of three lepton and quark families. The existence of families gives rise to many parameters of the standard model (SM). Flavor-changing neutral-currents (FCNC) induced B-meson rare decays provide an ideal opportunity for extracting information about the fundamental parameters of the SM, such as the Cabibbo-Kobayashi-Maskawa (CKM) matrix elements, and for testing the SM predictions at loop level and probing possible new physics. The experimental discovery of the inclusive and exclusive rare decays  $b \rightarrow X_s \gamma$  and  $B \rightarrow K \gamma$  [1] stimulated the study of radiative rare B-meson decays with a new momentum.

The inclusive decays  $B \rightarrow X_s \ell^+ \ell^-$  ( $\ell = e, \mu$ ) have been well studied in the frameworks of minimal supersymmetric model [2], the two Higgs doublet model (2HDM) [3–5] and the technicolor models [6,7]. It was shown that the matrix elements are strongly suppressed by a factor  $m_\ell/m_W$  and the contributions from exchanging neutral scalars can be safely neglected. However, the situation is different in the case of  $\ell = \tau$ . The branching ratio  $Br(B_s \rightarrow \tau^+ \tau^-) \simeq 8 \times 10^{-7}$  [8] in the SM is large enough to be observable in future B-factories. The contributions from neutral scalars exchange to  $B \rightarrow X_s \tau^+ \tau^-$  may no longer be negligible and thus also have to be examined.

On the other hand, among rare B-meson decays,  $B_s \rightarrow \tau^+ \tau^- \gamma$  is of special interest due to its relative cleanliness and sensitivity to models beyond the SM [9,10]. We emphasize that when photon is emitted in addition to the lepton pair, no helicity suppression exists, and “large” branching ratio is expected. As in the decay of  $B_s \rightarrow \tau^+ \tau^-$ , we could expect that for  $B_s \rightarrow \tau^+ \tau^- \gamma$  the contributions from exchanging scalars could be sizable.

In this work, we will study the inclusive and exclusive decays  $B \rightarrow X_s \tau^+ \tau^-$  and  $B_s \rightarrow \tau^+ \tau^- \gamma$  in technicolor model with scalars. Since several scalars are predicted in this model, they are expected to cause sizable effects in these decays. Taking into account the contributions from both the neutral and charged scalars predicted in this model, we will evaluate the branching ratios, the forward-backward asymmetry as well as the distributions of differential branching ratios. This paper is organized as follows. Section II is a brief review of the model. The detailed calculations of the contributions from the scalars are presented in Section III and IV for the decays  $B \rightarrow X_s \tau^+ \tau^-$  and  $B_s \rightarrow \tau^+ \tau^- \gamma$ , respectively. Finally, in Sec. V we give some numerical results and conclusions.

## II. TECHNICOLOR WITH SCALARS

In the technicolor model with scalars, the rare decay processes we will study receive contributions not only from the SM particles but also from charged and neutral physical scalars predicted in such a technicolor model. In this section we will briefly discuss the model and give the relevant Lagrangian which are needed in our calculation. More details of the model have been described in Refs. [11,12].

The gauge structure of the technicolor model with scalars is simply the direct product of the technicolor and standard model gauge groups:  $SU(N)_{TC} \times SU(3)_C \times SU(2)_W \times U(1)_Y$  [12]. The ordinary techni-singlet fermions are exactly as those in the SM. The technicolor sector consists of two techniflavors  $p$  and  $m$  that also transform under

$SU(2)_W$ . In addition to the above particle spectrum, there exists a scalar doublet  $\phi$  to which both the ordinary fermions and technifermions are coupled. Unlike the SM Higgs doublet,  $\phi$  does not cause electroweak symmetry breaking but obtains a non-zero effective vacuum expectation value (VEV) when technicolor breaks the symmetry.

Writing the matrix form of the scalar doublet as

$$\Phi = \begin{bmatrix} \bar{\phi}^0 & \phi^+ \\ -\phi^- & \phi^0 \end{bmatrix} \equiv \frac{(\sigma + f')}{\sqrt{2}} \Sigma', \quad (2.1)$$

we then have the kinetic terms for the scalar fields given by

$$\mathcal{L}_{K.E.} = \frac{1}{2} \partial_\mu \sigma \partial^\mu \sigma + \frac{1}{4} f^2 \text{Tr}(D_\mu \Sigma^\dagger D^\mu \Sigma) + \frac{1}{4} (\sigma + f')^2 \text{Tr}(D_\mu \Sigma'^\dagger D^\mu \Sigma'). \quad (2.2)$$

Here the non-linear representation  $\Sigma = \exp(\frac{2i\pi}{f})$  and  $\Sigma' = \exp(\frac{2i\pi'}{f'})$  are adopted for the technipion fields.  $\sigma$  is an isosinglet scalar field,  $f$  and  $f'$  are the technipion decay constant and the effective VEV, respectively. The covariant derivative is defined as  $D^\mu \Sigma = \partial^\mu \Sigma - ig W_\mu^a \frac{\tau_a}{2} \Sigma + ig' B_\mu \Sigma \frac{\tau_3}{2}$  with  $\tau_a/2$  ( $a = 1, 2, 3$ ) being the  $SU(2)$  generators, and  $W_\mu^a$  ( $B_\mu$ ) denote the  $SU(2)$  ( $U(1)$ ) vector fields with the gauge coupling constant  $g$  ( $g'$ ). The definition of  $D^\mu \Sigma'$  is analogous to that of  $D^\mu \Sigma$ .

The mixing between  $\pi$  and  $\pi'$  gives

$$\pi_a = \frac{f\pi + f'\pi'}{\sqrt{f^2 + f'^2}}, \quad (2.3)$$

$$\pi_p = \frac{-f'\pi + f\pi'}{\sqrt{f^2 + f'^2}}, \quad (2.4)$$

with  $\pi_a$  becoming the longitudinal component of the W and Z, and  $\pi_p$  remaining in the low-energy theory as an isotriplet of physical scalars. From Eq. (2.2) one can obtain the correct gauge boson masses providing that  $f^2 + f'^2 = V^2$  with the electroweak scale  $V = 246 \text{ GeV}$ .

Additionally, the contributions to scalar potential generated by the technicolor interactions should be included in this model. The simplest term one can construct is

$$\mathcal{L}_T = c_1 4\pi f^3 \text{Tr} \left[ \Phi \begin{pmatrix} h_+ & 0 \\ 0 & h_- \end{pmatrix} \Sigma^\dagger \right] + h.c., \quad (2.5)$$

where  $c_1$  is a coefficient of order unity,  $h_+$  and  $h_-$  are the Yukawa couplings of scalars to  $p$  and  $m$ . From Eq. (2.5) the mass of the charged scalar at lowest order is obtained as

$$m_{\pi_p}^2 = 2\sqrt{2}(4\pi f/f')v^2 h \quad (2.6)$$

with  $h = (h_+ + h_-)/2$ .

In general,  $f$  and  $f'$  depend on  $h_+$ ,  $h_-$ ,  $M_\phi$  and  $\lambda$ , where  $M_\phi$  is the mass of the scalar doublet  $\phi$ , and  $\lambda$  is  $\phi^4$  coupling. Two limits of the model have been studied previously in the literatures: (i) the limit in which  $\lambda$  is small and can be neglected [11], and (ii) the limit in which  $M_\phi$  is small and can be neglected [12]. When the largest Coleman-Weinberg corrections for the  $\sigma$  field are included in the effective chiral Lagrangian [12],  $M_\phi$ ,  $\lambda$  are replaced by the shifted scalar mass  $\tilde{M}_\phi$  and coupling  $\tilde{\lambda}$ . In this case, one obtains the constraint

$$\tilde{M}_\phi^2 f' + \frac{\tilde{\lambda}}{2} f'^3 = 8\sqrt{2}\pi c_1 h f^3 \quad (2.7)$$

and the isoscalar mass as

$$m_\sigma^2 = \tilde{M}_\phi^2 + \frac{2}{3\pi^2} [6(\frac{m_t}{f'})^4 + N h^4] f'^2 \quad (2.8)$$

in limit (i), and

$$m_\sigma^2 = \frac{3}{2} \tilde{\lambda} f'^2 - \frac{1}{4\pi^2} [6(\frac{m_t}{f'})^4 + N h^4] f'^2 \quad (2.9)$$

in limit (ii). The advantage of working in these two limits is that at the lowest order the phenomenology depends on  $h$ , not on the difference of  $h_+$  and  $h_-$ , and can be described in terms of  $(\tilde{M}_\phi, h)$  in limit (i) and  $(\tilde{\lambda}, h)$  in limit (ii). In this paper, we will work in the unitary gauge, where the particle spectrum consists of  $\pi_p$ ,  $\sigma$  and the massive weak gauge bosons. We choose two parameters  $(f/f', m_{\pi_p})$  in both limits of the model, and assume  $N = 4$ ,  $c_1 = 1$  in numerical calculations.

The interactions relevant to our calculations can be extracted from Eq. (2.2) and Eq. (2.5) and are given by

$$\begin{aligned}
\mathcal{L} = & \left(\frac{f}{f'}\right) \frac{gm_W}{2} \sigma W_\mu^+ W_\mu^- + \left(\frac{f'}{V}\right) \frac{gm_Z}{\cos\theta_W} \sigma Z^\mu Z_\mu - \left(\frac{f}{V}\right) \frac{g}{2} \sigma [W_\mu^- \partial^\mu \pi_p^+ + W_\mu^+ \partial^\mu \pi_p^-] \\
& + \left(\frac{V}{f'}\right) \frac{gm_{\pi_p}^2}{2m_W} \sigma \pi_p^+ \pi_p^- + \left(\frac{V}{f'}\right) \frac{ig}{2m_W} \sigma [m_U \bar{U}U + m_D \bar{D}D] \\
& + \frac{ig}{2} \left[ W_\mu^- \pi_p^+ \overset{\leftrightarrow}{\partial}^\mu \pi_p^0 + W_\mu^+ \pi_p^- \overset{\leftrightarrow}{\partial}^\mu \pi_p^0 \right] + \frac{ig \cos 2\theta_W}{2 \cos \theta_W} Z_\mu \pi_p^+ \overset{\leftrightarrow}{\partial}^\mu \pi_p^- \\
& - e A_\mu \pi_p^+ \overset{\leftrightarrow}{\partial}^\mu \pi_p^- + \left(\frac{f}{f'}\right) \frac{ig}{2m_W} \pi_p^0 [m_U \bar{U} \gamma_5 U - m_D \bar{D} \gamma_5 D] \\
& - \left(\frac{f}{f'}\right) \frac{ig}{2\sqrt{2}m_W} \{ \pi_p^+ \bar{U}_i [(m_U - m_D) - (m_U + m_D) \gamma_5] V_{ij} D_j \\
& \quad - \pi_p^- \bar{D}_i V_{ij}^* [(m_U - m_D) + (m_U + m_D) \gamma_5] U_j \} ,
\end{aligned} \tag{2.10}$$

where  $U$ ,  $D$  and  $m_U$ ,  $m_D$  represent the column vector and the diagonal mass matrix for up and down-quarks, respectively.  $\pi_p$  stands for the scalar field and  $V_{ij}$  are the elements of the CKM matrix. The physical scalar-lepton couplings can be read off from the expression above by replacing  $(U, D)$  with the corresponding lepton fields, replacing quark mass matrices with the corresponding diagonal lepton mass matrices, and setting  $V_{ij} = 1$ .

### III. $B \rightarrow X_s \tau^+ \tau^-$ IN TECHNICOLOR MODEL WITH SCALARS

It is well known that inclusive decay rates of heavy hadrons can be calculated in heavy quark effective theory [13], and the leading terms in  $1/m_Q$  expansion turn out to be the decay of a free heavy quark and corrections stem from the order  $1/m_Q^2$  [14]. In the technicolor model with scalars, the short distance contribution to  $b \rightarrow s \tau^+ \tau^-$  decay can be computed in the framework of the QCD corrected effective weak Hamiltonian, obtained by integrating out heavy particles, i.e., top quark, scalar  $\sigma$ ,  $\pi_p$  and  $W^\pm$ ,  $Z$  bosons

$$\mathcal{H}_{eff} = \frac{4G_F}{\sqrt{2}} V_{tb} V_{ts}^* \left( \sum_{i=1}^{10} [C_i(\mu) \mathcal{O}_i(\mu) + C_{Q_i}(\mu) \mathcal{Q}_i(\mu)] \right) , \tag{3.1}$$

where  $\mathcal{O}_i$  are the same as these given in Ref. [3]. The additional operators  $\mathcal{Q}_i$  [4] are due to the neutral scalars exchange diagrams, which give considerable contributions in the case that the final lepton pair is  $\tau^+ \tau^-$ . Here we only present the explicit expressions of the operators governing  $B \rightarrow X_s \tau^+ \tau^-$ . They read

$$\begin{aligned}
\mathcal{O}_7 &= \frac{e}{16\pi^2} m_b (\bar{s}_\alpha \sigma^{\mu\nu} R b_\alpha) F_{\mu\nu}, \\
\mathcal{O}_8 &= \frac{e}{16\pi^2} (\bar{s}_\alpha \gamma^\mu L b_\alpha) (\bar{\tau} \gamma_\mu \tau), \\
\mathcal{O}_9 &= \frac{e}{16\pi^2} (\bar{s}_\alpha \gamma^\mu L b_\alpha) (\bar{\tau} \gamma_\mu \gamma_5 \tau), \\
\mathcal{Q}_1 &= \frac{e^2}{16\pi^2} (\bar{s}_\alpha R b_\alpha) (\bar{\tau} \gamma_\mu \tau), \\
\mathcal{Q}_2 &= \frac{e^2}{16\pi^2} (\bar{s}_\alpha R b_\alpha) (\bar{\tau} \gamma_\mu \gamma_5 \tau) ,
\end{aligned} \tag{3.2}$$

where  $L, R = (1 \mp \gamma_5)/2$ ,  $\alpha$  is the SU(3) color index and  $F^{\mu\nu}$  the field strength tensor of the electromagnetic interaction.

In general in theories beyond the SM there will be additional contributions, which are characterized by the values of the coefficients  $C_i$  and  $C_{Q_i}$  at the perturbative scale  $m_W$ . Using the Feynman rules presented in the preceding section, we can calculate the additional contributions arising from the scalars  $\sigma$ ,  $\pi_p^0$  and  $\pi_p^\pm$ . At the scale of  $m_W$ ,

the Feynman diagrams for the charged scalar contributions are depicted in Fig. 1, while Fig. 2 shows the additional contributions from the neutral scalars.

The contributions of Fig. 1 to the Wilson coefficients at leading order read<sup>1</sup>

$$\begin{aligned} C_7(m_W)_{TC} &= \left(\frac{f}{f'}\right)^2 H_1(x_{\pi_p}), \\ C_8(m_W)_{TC} &= \left(\frac{f}{f'}\right)^2 \frac{4\sin^2\theta_W - 1}{\sin^2\theta_W} [x_W H_2(x_{\pi_p}) - x_{\pi_p} H_3(x_{\pi_p})], \\ C_9(m_W)_{TC} &= \left(\frac{f}{f'}\right)^2 \frac{x_W}{\sin^2\theta_W} H_2(x_{\pi_p}), \end{aligned} \quad (3.3)$$

where  $x_i = m_i^2/m_t^2$ ,  $\theta_W$  is the Weinberg angle and the functions  $H_i$  can be expressed as

$$\begin{aligned} H_1(x) &= \frac{x}{12(x-1)^3} \left[ \frac{22x^2 - 53x + 25}{6} - \frac{3x^2 - 8x + 4}{x-1} \ln x \right], \\ H_2(x) &= \frac{x}{8(x-1)} \left[ -1 + \frac{1}{x-1} \ln x \right], \\ H_3(x) &= \frac{1}{18(x-1)^3} \left[ \frac{47x^2 - 79x + 38}{6} - \frac{3x^3 - 6x + 4}{x-1} \ln x \right]. \end{aligned} \quad (3.4)$$

Theoretical calculations show that the contributions of Fig. 2 are significant only for large  $f/f'$ . Keeping only the leading terms in large  $f/f'$  limit, the  $C_{Q_i}(m_W)$  induced from these diagrams are given by

$$\begin{aligned} C_{Q_1}(m_W) &= -\left(\frac{f}{f'}\right)^4 \frac{m_b m_\tau}{m_\sigma^2} \frac{x_W}{4\sin^2\theta_W} H_4(x_{\pi_p}), \\ C_{Q_2}(m_W) &= -\left(\frac{f}{f'}\right)^4 \frac{m_b m_\tau}{m_{\pi_p}^2} \frac{x_W}{4\sin^2\theta_W} H_5(x_{\pi_p}), \end{aligned} \quad (3.5)$$

with

$$\begin{aligned} H_4(x) &= \frac{1}{2(x-1)^2} \left[ \frac{4x^2 - 7x + 1}{2} - \frac{x^2 - 2x}{x-1} \ln x \right], \\ H_5(x) &= \frac{1}{(x-1)} \left[ \frac{x+1}{2} - \frac{x}{x-1} \ln x \right]. \end{aligned} \quad (3.6)$$

It is noticeable that the contributions of Fig. 2 are proportional to  $(f/f')^4$ , while those of Fig. 1 proportional to  $(f/f')^2$ . So for a sufficiently large  $f/f'$ , the contributions of neutral scalars in Fig. 2 are relatively enhanced and become comparable with those from charged scalars in Fig. 1.

Neglecting the strange quark mass, the effective Hamiltonian (3.1) leads to the following matrix element for the inclusive  $b \rightarrow s\tau^+\tau^-$  decay,

$$\begin{aligned} \mathcal{M} &= \frac{\alpha_{em} G_F}{2\sqrt{2}\pi} V_{tb} V_{ts}^* \left\{ -2C_7^{eff} \frac{m_b}{p^2} \bar{s} i\sigma_{\mu\nu} p_\nu (1 + \gamma_5) b \right. \\ &\quad + C_8^{eff} \bar{s} \gamma_\mu (1 - \gamma_5) b \bar{\tau} \gamma_\mu \tau + C_9 \bar{s} \gamma_\mu (1 - \gamma_5) b \bar{\tau} \gamma_\mu \gamma_5 \tau \\ &\quad \left. + C_{Q_1} \bar{s} (1 + \gamma_5) b \bar{\tau} \tau + C_{Q_2} \bar{s} (1 + \gamma_5) b \bar{\tau} \gamma_5 \tau \right\}. \end{aligned} \quad (3.7)$$

The Wilson coefficients  $C_i$ ,  $C_{Q_j}$  are to be evaluated from  $m_W$  down to the lower scale of about  $m_b$  by using the renormalization group equation. When evolving down to  $b$  quark scale, the operators  $\mathcal{O}_{1,2}$  and  $\mathcal{Q}_3$  can mix with  $\mathcal{O}_i$ , ( $i = 7, 8$ ); however, they can be included in an “effective”  $\mathcal{O}_{7,8}$  because of their same structures contributing to the  $b \rightarrow s\tau^+\tau^-$  matrix element. At leading order, the Wilson coefficients are [3–5]

---

<sup>1</sup> The contributions of  $\pi_p^\pm$  take a similar form from those contributions of the color-singlet charged pseudo-Goldstone boson in the one-generation technicolor model [15]. The typical difference is the factor  $f/f'$  in these new contributions.

$$C_7^{eff}(m_b) = \eta^{-16/23} \left\{ C_7(m_W) - \left[ \frac{58}{135}(\eta^{10/23} - 1) + \frac{29}{189}(\eta^{28/23} - 1) \right] C_2(m_W) - 0.012 C_{Q_3}(m_W) \right\}, \quad (3.8)$$

$$C_8^{eff}(m_b) = C_8(m_W) + \frac{4\pi}{\alpha_s(m_b)} \left[ \frac{4}{33}(\eta^{-11/23} - 1) + \frac{8}{87}(1 - \eta^{-29/23}) \right] \\ + \left\{ g\left(\frac{m_c^2}{m_b^2}, \frac{p^2}{m_b^2}\right) - \frac{3\pi}{\alpha_{em}^2} \kappa \sum_{V_i=\Psi', \Psi'', \dots} \frac{m_{V_i} \Gamma(V_i \rightarrow \tau^+ \tau^-)}{m_{V_i}^2 - p^2 - i m_{V_i} \Gamma_{V_i}} \right\} [3C_1(m_b) + C_2(m_b)], \quad (3.9)$$

$$C_9(m_b) = C_9(m_W), \quad (3.10)$$

$$C_{Q_i}(m_b) = \eta^{-\gamma_Q/\beta_0} C_{Q_i}(m_W). \quad (3.11)$$

Here  $p$  is the momentum transfer, and

$$C_{Q_3}(m_W) = \frac{m_b e^2}{m_\tau g^2} [C_{Q_1}(m_W) + C_{Q_2}(m_W)], \quad (3.12)$$

where  $\gamma_Q = -4$  is the anomalous dimension of  $\bar{s} R b$ ,  $\beta_0 = 11 - 2n_f/3$ ,  $\eta = \alpha_s(m_b)/\alpha_s(m_W)$ ,  $C_2(m_W) = 1$  and  $C_{1,2}(m_b) = (\eta^{-6/23} \mp \eta^{12/23})/2$ .  $g(m_c^2/m_b^2, s)$  in Eq. (3.9) arises from the one-loop matrix elements of the four-quark operators, and

$$g(x, y) = -\frac{4}{9} \ln x + \frac{8}{27} + \frac{16x}{9y} - \frac{4}{9} \left(1 + \frac{2x}{y}\right) \left|1 - \frac{4x}{y}\right|^{1/2} \begin{cases} \ln Z(x, y) - i\pi & \text{for } 4x/y < 1 \\ 2 \arctan \frac{1}{\sqrt{4x/y - 1}} & \text{for } 4x/y > 1 \end{cases} \quad (3.13)$$

where

$$Z(x, y) = \frac{1 + \sqrt{1 - \frac{4x}{y}}}{1 - \sqrt{1 - \frac{4x}{y}}}. \quad (3.14)$$

The second term in brace of Eq. (3.9) estimates the long-distance contribution from the intermediate  $\Psi', \Psi'', \dots$  [3]. The phenomenological parameter  $\kappa$  is taken as 2.3 [16] in our numerical calculations.

The formula of invariant dilepton mass distribution has been derived in [4], which is given by

$$\frac{d\Gamma(B \rightarrow X_s \tau^+ \tau^-)}{ds} = Br(B \rightarrow X_c \ell \nu) \frac{\alpha_{em}^2}{4\pi^2} \left| \frac{V_{tb} V_{ts}^*}{V_{cb}} \right|^2 f^{-1}(m_c/m_b) (1-s)^2 \left(1 - \frac{4r}{s}\right)^{1/2} D(s) \quad (3.15)$$

with

$$D(s) = 4|C_7^{eff}|^2 \left(1 + \frac{2r}{s}\right) \left(1 + \frac{2}{s}\right) + |C_8^{eff}|^2 \left(1 + \frac{2r}{s}\right) (1+2s) + |C_9|^2 (1-8r+2s+\frac{2r}{s}) \\ + 12Re(C_7^{eff} C_8^{eff*}) \left(1 + \frac{2r}{s}\right) + \frac{3}{2} |C_{Q_1}|^2 (s-4r) + \frac{3}{2} |C_{Q_2}|^2 s + 6Re(C_9 C_{Q_2}^*) r^{1/2}. \quad (3.16)$$

Here  $s = p^2/m_b^2$ ,  $r = m_\tau^2/m_b^2$ . Function  $f(x) = 1 - 8x^2 + 8x^6 - x^8 - 24x^4 \ln x$  is the phase-space factor.

The angular information and the forward-backward asymmetry are also sensitive to the details of the new physics. Defining the forward-backward asymmetry as

$$A_{FB}(s) = \frac{\int_0^1 d\cos\theta (d^2\Gamma/dsd\cos\theta) - \int_{-1}^0 d\cos\theta (d^2\Gamma/dsd\cos\theta)}{\int_0^1 d\cos\theta (d^2\Gamma/dsd\cos\theta) + \int_{-1}^0 d\cos\theta (d^2\Gamma/dsd\cos\theta)}, \quad (3.17)$$

where  $\theta$  is the angle between the momentum of B-meson and  $\tau^+$  in the center of mass frame of the dilepton, we obtain

$$A_{FB} = \frac{6(1-4r/s)^{1/2}}{D(s)} Re(2C_7^{eff} C_9^* + C_8^{eff} C_9^* s + 2C_7^{eff} C_{Q_2}^* r^{1/2} + C_8^{eff} C_{Q_1}^* r^{1/2}). \quad (3.18)$$

#### IV. $B_s \rightarrow \tau^+ \tau^- \gamma$ IN TECHNICOLOR MODEL WITH SCALARS

Now let us turn to rare radiative decay  $B_s \rightarrow \tau^+ \tau^- \gamma$ . The exclusive decay can be obtained from the inclusive decay  $b \rightarrow s \tau^+ \tau^- \gamma$ , and further, from  $b \rightarrow s \tau^+ \tau^-$ . To achieve this, it is necessary to attach photon to any charged internal and external lines in the Feynman diagrams of  $b \rightarrow s \tau^+ \tau^-$ . As pointed out in Ref. [9], contributions coming from the attachment of photon to any charged internal line are strongly suppressed and we can neglect them safely. However, since the mass of  $\tau$ -lepton is not much smaller than that of  $B_s$ -meson, in  $B_s \rightarrow \tau^+ \tau^- \gamma$  decay, the contributions of the diagrams with photon radiating from final leptons are comparable with those from initial quarks. When a photon is attached to the initial quark lines, the corresponding matrix element for the  $B_s \rightarrow \tau^+ \tau^- \gamma$  decay can be written as

$$\mathcal{M}_1 = \frac{\alpha_{em}^{3/2} G_F}{\sqrt{2}\pi} V_{tb} V_{ts}^* \{ [A \varepsilon_{\mu\alpha\beta\sigma} \epsilon_\alpha^* p_\beta q_\sigma + iB(\epsilon_\mu^*(pq) - (\epsilon^* p)q_\mu)] \bar{\tau} \gamma_\mu \tau + [C \varepsilon_{\mu\alpha\beta\sigma} \epsilon_\alpha^* p_\beta q_\sigma + iD(\epsilon_\mu^*(pq) - (\epsilon^* p)q_\mu)] \bar{\tau} \gamma_\mu \gamma_5 \tau \}, \quad (4.1)$$

where

$$\begin{aligned} A &= \frac{1}{m_{B_s}^2} [C_8^{eff} g_1(p^2) - 2C_7 \frac{m_b}{p^2} g_2(p^2)], \\ B &= \frac{1}{m_{B_s}^2} [C_8^{eff} f_1(p^2) - 2C_7 \frac{m_b}{p^2} f_2(p^2)], \\ C &= \frac{C_9}{m_{B_s}^2} g_1(p^2), \\ D &= \frac{C_9}{m_{B_s}^2} f_1(p^2). \end{aligned} \quad (4.2)$$

In obtaining Eq. (4.1) we have used

$$\langle \gamma | \bar{s} \gamma_\mu (1 \pm \gamma_5) | B_s \rangle = \frac{e}{m_{B_s}^2} \{ \varepsilon_{\mu\alpha\beta\sigma} \epsilon_\alpha^* p_\beta q_\sigma g_1(p^2) \mp i[(\epsilon_\mu^*(pq) - (\epsilon^* p)q_\mu)] f_1(p^2) \}, \quad (4.3)$$

$$\langle \gamma | \bar{s} i \sigma_{\mu\nu} p_\nu (1 \pm \gamma_5) b | B_s \rangle = \frac{e}{m_{B_s}^2} \{ \varepsilon_{\mu\alpha\beta\sigma} \epsilon_\alpha^* p_\beta q_\sigma g_2(p^2) \pm i[(\epsilon_\mu^*(pq) - (\epsilon^* p)q_\mu)] f_2(p^2) \}, \quad (4.4)$$

and

$$\langle \gamma | \bar{s} (1 \pm \gamma_5) | B_s \rangle = 0. \quad (4.5)$$

Here  $\epsilon_\mu$  and  $q_\mu$  are the four vector polarization and momentum of photon, respectively;  $g_i$ ,  $f_i$  are form factors [8,18]. Eq. (4.5) can be obtained by multiplying  $p_\mu$  in both sides of Eq. (4.4) and using the equations of motion. From Eq. (4.5) one can see that the neutral scalars do not contribute to the matrix element  $\mathcal{M}_1$ .

When a photon is radiated from the final  $\tau$ -leptons, the situation is different. Using the expressions

$$\begin{aligned} \langle 0 | \bar{s} b | B_s \rangle &= 0, \\ \langle 0 | \bar{s} \sigma_{\mu\nu} (1 + \gamma_5) b | B_s \rangle &= 0, \\ \langle 0 | \bar{s} \gamma_\mu \gamma_5 | B_s \rangle &= -i f_{B_s} P_{B_s \mu} \end{aligned} \quad (4.6)$$

and the conservation of the vector current, one finds that only the operators  $\mathcal{Q}_{1,2}$  and  $\mathcal{O}_9$  give contribution to this Bremsstrahlung part. The corresponding matrix is given by [10]

$$\begin{aligned} \mathcal{M}_2 &= \frac{\alpha_{em}^{3/2} G_F}{\sqrt{2}\pi} V_{tb} V_{ts}^* i 2m_\tau f_{B_s} \left\{ (C_9 + \frac{m_{B_s}^2}{2m_\tau m_b} C_{Q_2}) \bar{\tau} \left[ \frac{\not{\epsilon} \not{P}_{B_s}}{2p_1 q} - \frac{\not{P}_{B_s} \not{\epsilon}}{2p_2 q} \right] \gamma_5 \tau \right. \\ &\quad \left. + \frac{m_{B_s}^2}{2m_\tau m_b} C_{Q_1} \left[ 2m_\tau \left( \frac{1}{2p_1 q} + \frac{1}{2p_2 q} \right) \bar{\tau} \not{\epsilon} \tau + \bar{\tau} \left( \frac{\not{\epsilon} \not{P}_{B_s}}{2p_1 q} - \frac{\not{P}_{B_s} \not{\epsilon}}{2p_2 q} \right) \gamma_5 \tau \right] \right\}. \end{aligned} \quad (4.7)$$

Here  $P_{B_s}$ ,  $f_{B_s}$  are the momentum and the decay constant of the  $B_s$  meson.

Finally, the total matrix element for the  $B_s \rightarrow \tau^+ \tau^- \gamma$  decay is obtained as a sum of the  $\mathcal{M}_1$  and  $\mathcal{M}_2$ . After summing over the spins of the  $\tau$ -leptons and polarization of the photon, we get the square of the matrix element as

$$|\mathcal{M}|^2 = |\mathcal{M}_1|^2 + |\mathcal{M}_2|^2 + 2Re(\mathcal{M}_1 \mathcal{M}_2^*) \quad (4.8)$$

with<sup>2</sup>

$$\begin{aligned}
|\mathcal{M}_1|^2 = & 4 \left| \frac{\alpha_{em}^{3/2} G_F}{\sqrt{2}\pi} V_{tb} V_{ts}^* \right|^2 \{ [|A|^2 + |B|^2] [p^2((p_1 q)^2 + (p_2 q)^2) + 2m_\tau^2(pq)^2] \\
& + [|C|^2 + |D|^2] [p^2((p_1 q)^2 + (p_2 q)^2) - 2m_\tau^2(pq)^2] \\
& + 2\text{Re}(B^* C + A^* D) p^2((p_1 q)^2 - (p_2 q)^2) \}, \tag{4.9}
\end{aligned}$$

$$\begin{aligned}
2\text{Re}(\mathcal{M}_1 \mathcal{M}_2^*) = & -16 \left| \frac{\alpha_{em}^{3/2} G_F}{\sqrt{2}\pi} V_{tb} V_{ts}^* \right|^2 m_\tau^2 f_{B_s}(pq)^2 \left\{ \left| C_9 + \frac{m_{B_s}^2 C_{Q_2}}{2m_\tau m_b} \right| \left[ \text{Re}(A) \frac{(p_1 q + p_2 q)}{(p_1 q)(p_2 q)} \right. \right. \\
& \left. \left. - \text{Re}(D) \frac{(p_1 q - p_2 q)}{(p_1 q)(p_2 q)} \right] + \text{Re}(B) \left| \frac{m_{B_s}^2 C_{Q_1}}{2m_\tau m_b} \right| \left[ \frac{3m_{B_s}^2 + 2m_\tau^2 - 5(pq)}{(p_1 q)(p_2 q)} - \frac{2p^2}{(pq)^2} \right] \right. \\
& \left. + \text{Re}(C) \left| \frac{m_{B_s}^2 C_{Q_1}}{2m_\tau m_b} \right| \left[ \frac{(p_1 q - p_2 q)}{(p_1 q)(p_2 q)} \left( 1 + \frac{2p^2}{(pq)^2} \right) \right] \right\}, \tag{4.10}
\end{aligned}$$

$$\begin{aligned}
|\mathcal{M}_2|^2 = & -8 \left| \frac{\alpha_{em}^{3/2} G_F}{\sqrt{2}\pi} V_{tb} V_{ts}^* \right|^2 m_\tau^2 f_{B_s}^2 \left\{ \left| C_9 + \frac{m_{B_s}^2 C_{Q_2}}{2m_\tau m_b} \right|^2 \left[ \frac{m_\tau^2 m_{B_s}^2 (pq)^2}{(p_1 q)^2 (p_2 q)^2} - \frac{m_{B_s}^2 p^2 + 2(pq)^2}{(p_1 q)(p_2 q)} \right] \right. \\
& \left. - \left| \frac{m_{B_s}^2 C_{Q_1}}{2m_\tau m_b} \right|^2 \left[ \frac{m_\tau^2 (m_{B_s}^2 - 4m_\tau^2)(pq)^2}{(p_1 q)^2 (p_2 q)^2} - \frac{(m_{B_s}^2 - 4m_\tau^2)p^2 + 2(pq)^2}{(p_1 q)(p_2 q)} \right] \right\}. \tag{4.11}
\end{aligned}$$

Here  $p_1, p_2$  are momenta of the final  $\tau$ -leptons. It is obvious that the quantity  $|\mathcal{M}|^2$  depends only on the scalar products of the momenta of the external particles.

In the rest frame of the  $B_s$ , the photon energy  $E_\gamma$  and the lepton energy  $E_1$  are restricted by

$$\begin{aligned}
0 \leq E_\gamma \leq & \frac{m_{B_s}^2 - 4m_\tau^2}{2m_{B_s}}, \\
\frac{m_{B_s} - E_\gamma}{2} - \frac{E_\gamma}{2} \sqrt{1 - \frac{4m_\tau^2}{m_{B_s}^2 - 2m_{B_s} E_\gamma}} \leq E_1 \leq & \frac{m_{B_s} - E_\gamma}{2} + \frac{E_\gamma}{2} \sqrt{1 - \frac{4m_\tau^2}{m_{B_s}^2 - 2m_{B_s} E_\gamma}}. \tag{4.12}
\end{aligned}$$

However, in  $|\mathcal{M}_2|^2$  it appears an infrared divergence, which originates in the Bremsstrahlung processes when photon is soft and in this case, the  $B_s \rightarrow \tau^+ \tau^- \gamma$  can not be distinguished from  $B_s \rightarrow \tau^+ \tau^-$ . Therefore, both processes must be considered together in order to cancel the infrared divergence. Taking the fact that the infrared singular terms in  $|\mathcal{M}_2|^2$  exactly cancel the  $O(\alpha_{em})$  virtual correction in  $B_s \rightarrow \tau^+ \tau^-$  amplitude in account [9], we follow Ref. [9] and consider the photon in  $B_s \rightarrow \tau^+ \tau^- \gamma$  as a hard photon and impose a cut on the photon energy  $E_\gamma$ , which correspond to the radiated photon can be detected in the experiments. This cut requires  $E_\gamma \geq \delta m_{B_s}/2$  with  $\delta = 0.02$ .

After integrating over the phase space and the lepton energy  $E_1$ , we express the decay rate as

$$\begin{aligned}
\Gamma = & \left| \frac{\alpha_{em}^{3/2} G_F}{2\sqrt{2}\pi} V_{tb} V_{ts}^* \right|^2 \frac{m_{B_s}^5}{(2\pi)^3} \left\{ \frac{m_{B_s}^2}{12} \int_{4\hat{r}}^{1-\delta} (1-\hat{s})^3 d\hat{s} \sqrt{1 - \frac{4\hat{r}}{\hat{s}}} [ (|A|^2 + |B|^2)(\hat{s} + 2\hat{r}) \right. \\
& + (|C|^2 + |D|^2)(\hat{s} - 4\hat{r}) ] - 2f_{B_s} |C_9 + \frac{m_{B_s}^2 C_{Q_2}}{2m_\tau m_b}| \hat{r} \int_{4\hat{r}}^{1-\delta} (1-\hat{s})^2 d\hat{s} \text{Re}(A) \ln \hat{z} \\
& - 2f_{B_s} \left| \frac{m_{B_s}^2 C_{Q_1}}{2m_\tau m_b} \right| \hat{r} \int_{4\hat{r}}^{1-\delta} (1-\hat{s}) d\hat{s} \text{Re}(B) \left[ (1 + 4\hat{r} + 5\hat{s}) \ln \hat{z} + \hat{s} \sqrt{1 - \frac{4\hat{r}}{\hat{s}}} \right] \\
& - \frac{4f_{B_s}^2}{m_{B_s}^2} |C_9 + \frac{m_{B_s}^2 C_{Q_2}}{2m_\tau m_b}|^2 \hat{r} \int_{4\hat{r}}^{1-\delta} d\hat{s} \left[ (1 + \hat{s} + \frac{4\hat{r} - 2}{1 - \hat{s}}) \ln \hat{z} + \frac{2\hat{s}}{1 - \hat{s}} \sqrt{1 - \frac{4\hat{r}}{\hat{s}}} \right] \\
& \left. + f_{B_s}^2 \left| \frac{C_{Q_1}}{m_b} \right|^2 \int_{4\hat{r}}^{1-\delta} d\hat{s} \left[ (1 - 8\hat{r} + \hat{s} - \frac{2 - 10\hat{r} + 8\hat{r}^2}{1 - \hat{s}}) \ln \hat{z} + \frac{2(1 - 4\hat{r})\hat{s}}{1 - \hat{s}} \sqrt{1 - \frac{4\hat{r}}{\hat{s}}} \right] \right\}, \tag{4.13}
\end{aligned}$$

---

<sup>2</sup>There are some errors in Eqs. (15) and (17) of Ref. [10]. We believe the expressions of  $C_{Q_1}^H(m_W)$  and  $C_{Q_2}^H(m_W)$  are not correct in Two-Higgs-Double model I.

where  $\hat{s} = p^2/m_{B_s}^2$ ,  $\hat{r} = m_\tau^2/m_{B_s}^2$ .  $\hat{z} \equiv Z(\hat{r}, \hat{s})$  takes the form given in Eq. (3.14).

## V. NUMERICAL RESULTS AND CONCLUSION

In this section we give some numerical results and discussions. For reference, we present our SM predictions<sup>3</sup>

$$\begin{aligned} Br(B \rightarrow X_s \tau^+ \tau^-) &= 2.59 \times 10^{-6}, \\ Br(B_s \rightarrow \tau^+ \tau^- \gamma) &= 5.18 \times 10^{-8}. \end{aligned} \quad (5.1)$$

These values are obtained for the fixed input parameters [17] listed in Table I and the QCD coupling constant  $\alpha_s(m_b) = 0.218$  which is calculated via

$$\alpha_s(\mu) = \frac{\alpha_s(m_Z)}{1 - \beta_0 \frac{\alpha_s(m_Z)}{2\pi} \ln \frac{m_Z}{\mu}} \quad (5.2)$$

with  $\alpha_s(m_Z) = 0.119$  [17] and  $m_Z = 91.19 \text{ GeV}$ .

Table I. The value of the input parameters used in the numerical calculations (mass and decay constant in unit GeV).

$m_t$	$m_c$	$m_b$	$m_\tau$	$m_{B_s}$	$m_W$
176	1.4	4.8	1.78	5.26	80.448
$f_{B_s}$ [19]	$ V_{tb}V_{ts}^* $	$ V_{tb}V_{ts}^*/V_{cb} ^2$	$\alpha_{em}^{-1}$	$\tau(B_s)$	$\sin^2 \theta_W$
0.14	0.045	0.95	137	$1.64 \times 10^{-12} \text{ s}$	0.2325

In addition, we use the masses, decay widths and branching rates of  $J/\Psi$  family in Ref. [17], the normalized factor, branching rate  $Br(B \rightarrow X_c \ell \nu) = 10.2\%$ , and take the dipole forms of the form-factors given by Ref. [18]

$$\begin{aligned} g_1(p^2) &= \frac{1 \text{ GeV}}{(1 - p^2/5.6^2)^2}, & g_2(p^2) &= \frac{3.74 \text{ GeV}}{(1 - p^2/40.5^2)^2}, \\ f_1(p^2) &= \frac{0.8 \text{ GeV}}{(1 - p^2/6.5^2)^2}, & f_2(p^2) &= \frac{0.68 \text{ GeV}}{(1 - p^2/30)^2}. \end{aligned} \quad (5.3)$$

As mentioned in Sec. II, in limit (i) and (ii) there are only two independent parameters  $f/f'$  and  $m_{\pi_p}$  in technicolor model with scalars. The limit on  $f/f'$  can be obtained from the studies of  $b \rightarrow X_c \tau \nu$  [20],  $b \rightarrow X_s \gamma$  [20,21],  $Z \rightarrow b\bar{b}$  [21],  $B \rightarrow X_s \mu^+ \mu^-$  [22] and B- $\bar{B}$  mixing in technicolor model with scalars [11,12,21], which is given by [20]

$$\frac{f}{f'} \leq 0.03 \left( \frac{m_{\pi_p}}{1 \text{ GeV}} \right) \quad (95\% \text{ C. L.}) \quad (5.4)$$

This indicates that  $f/f'$  could be large for large  $m_{\pi_p}$ . On the other hand, we should notice the induced values of  $m_\sigma$  in Eqs. (2.8, 2.9). Although the lower experimental bound of  $107.7 \text{ GeV}$  [17] on the SM Higgs boson may not be applied directly to  $m_\sigma$ , we ensure that the neutral scalar  $\sigma$  is not lighter than this value in our numerical calculations.

We found that the behaviors of the quantities we studied are similar in limit (i) and (ii). So for illustrations, we only present some numerical results in limit (ii). Some numerical examples are presented in Figs. 3-6.

Fig. 3 and Fig. 4 show the branching ratios of  $B \rightarrow X_s \tau^+ \tau^-$  and  $B_s \rightarrow \tau^+ \tau^- \gamma$ , respectively. As expected, the branching ratios drop with  $m_{\pi_p}$  and increase with  $f/f'$ . For the specified values of  $m_{\pi_p}$  and  $f/f'$  in the figures, the branching ratios can be enhanced over the SM results by a couple of orders of magnitude.

---

<sup>3</sup>Switching off the scalars contributions, our formula for  $Br(B_s \rightarrow \tau^+ \tau^-)$  is the same as given in Ref. [9], but different from their result. In fact, the Bremsstrahlung part is  $3.98 \times 10^{-8}$  for  $\delta = 0.02$ .



Fig. 5 show the forward-backward (FB) asymmetry as a function of the scaled invariant dilepton mass squared  $s$ . We should point out that since some common contributions appearing in both the numerator and the denominator cancel out to some extent, the FB asymmetry is a sensitive, relatively model-independent probe of these models <sup>4</sup>. Fig. 5 shows a significant difference between the SM and the technicolor predictions, especially in the region of large invariant dilepton mass. One can see that, unlike the branching ratio, the forward-backward asymmetry is enhanced significantly due to the neutral scalars contributions.

The differential branching ratios of  $B \rightarrow X_s \tau^+ \tau^-$  and  $B_s \rightarrow \tau^+ \tau^- \gamma$  versus the scaled invariant dilepton mass squared are shown in Fig. 6. such distributions also differ significantly from the SM predictions. We stress that all these distributions would be useful for fitting the future experimental results in the framework of such a technicolor model, especially when some deviations from the SM predictions are discovered in future experiments. Different models, such as technicolor models and 2HDM's, may all predict same enhancements in branching ratios, but they may give different behaviors for some distributions. To claim a given model is experimentally favored or disfavored, all these distributions would be useful.

We realized that since there are new model assumptions introduced here, such as the form-factor (5.3), as well as a large number of experimental inputs, each of which comes with its own uncertainty, our conclusions may only be qualitatively reliable. These are:

1. The branching ratios predicted by the technicolor model with scalars can be enhanced over the SM results by a couple of orders of magnitude in parameter space we studied.
2. The dominant contributions are from the exchange of charged scalars as shown in Fig. 1. This could be well understood since the contributions from the charged scalars, in contrast to the decays studied in 2HDM-II [10], are not suppressed but enhanced by a factor  $(f/f')^2$  when  $f/f'$  is large.
3. The neutral scalars play no important role except for sufficiently large  $f/f'$ . For the illustrative values in the numerical results, i.e.,  $10 \leq f/f' \leq 15$ , the contributions of neutral scalars are still much smaller than those of charged scalars. However, as showed in the analytical expressions, the contributions of neutral scalars in Fig. 2 are two orders higher in  $f/f'$  than those of charged scalars in Fig. 1. Therefore, for sufficiently large  $f/f'$  the contributions of neutral scalars could also be important.
4. The possible large enhancements over those predicted by the SM might be detectable in future experiments since the sensitivity of the new generation of B experiment to these processes should be quite high. If such large enhancements are observed in future experiments, they could be interpreted in such a technicolor model although this model might not be the unique one to explain them. If not observed, further stringent constraints on the model parameter space could be obtained and thus this model would be severely disfavored.

## ACKNOWLEDGMENT

We thank C.-H. Chang and H. J. Yang for discussions and comments. This work is supported in part by a grant of Chinese Academy of Science for Outstanding Young Scholars.

- 
- [1] R. Ammar, *et al.*, CLEO Collaboration, Phys. Rev. Lett. **71**, 674 (1993); M. S. Alam *et al.*, CLEO Collaboration, Phys. Rev. Lett. **74**, 2885 (1995).
  - [2] Y. Grossman, Z. Ligeti, and E. Nardi, Phys. Rev. **D55**, 2768 (1997).
  - [3] B. Grinstein, R. Springer, and M. B. Wise, Phys. Lett. **B202**, 138 (1988); Nucl. Phys. **B339**, 269 (1990).
  - [4] Y. B. Dai, C. S. Huang and H. W. Huang, Phys. Lett. **B390**, 257 (1997).
  - [5] J. L. Hewett, Phys. Rev. **D53**, 4964 (1996).
  - [6] S. Weinberg, Phys. Rev. **D19**, 1277 (1979); L. Susskind, Phys. Rev. **D 20**, 2619 (1979).
  - [7] S. Dimopoulos and L. Susskind, Nucl. Phys. **B 155**, 237 (1979); E. Eichten and K. Lane, Phys. Lett. **B 90**, 125 (1980).
  - [8] G. Buchalla and A. J. Buras, Nucl. Phys. **B400**, 225 (1993); D. Du, C. Liu and D. Zhang, Phys. Lett. **B 317**, 179 (1993).
- 

<sup>4</sup>Although the FB asymmetry is less model-dependent for this reason, it is not completely model-independent since the model-dependent contributions cannot completely cancel out.

- [9] T. M. Aliev, A. ÖZpineci and M. Savci, Phys. Rev. D **55**, 7059 (1997); T. M. Aliev, N. K. Pak and M. Savci, Phys. Lett. B **424**, 175 (1998).
- [10] E. O. Iltan and G. Turan, Phys. Rev. D **61**, 034010 (2000).
- [11] E. H. Simmons, Nucl. Phys. B **312**, 253 (1989).
- [12] C. D. Carone and E. H. Simmons, Nucl. Phys. B **397**, 591 (1993); C. D. Carone and H. Georgi, Phys. Rev. D **49**, 1427 (1994).
- [13] M. Neubert, Phys. Rep. **245**, 396 (1994).
- [14] A. Falk, M. Misiak, and M. Muñiz, Nucl. Phys. B **49**, 3367 (1994); A. Falk, M. Luke, and M. Savage, Phys. Rev. D **53**, 2491 (1996); I. Bigi, M. Shifman, N. G. Uraltsev, and A. I. Vainshtein, Phys. Rev. Lett. **71**, 496 (1993); A. V. Manohar and M. B. Wise, Phys. Rev. D **49**, 1310 (1994).
- [15] G. Lu, Z. Xiong and Y. Cao, Nucl. Phys. B **487**, 43 (1997).
- [16] A. Ali and C. Creub, Z. Phys. C **49**, 431 (1991); Phys. Lett. B **259**, 182 (1991); **361**, 146 (1995).
- [17] Particle Physics Group. Eur. Phys. J. C 1998, **15**, 274 (2000).
- [18] G. Eilam, I. Halperin and R. R. Mendel, Phys. Lett. B **361**, 137 (1995).
- [19] V. M. Belyaev *et al.*, Phys. Rev. D **51**, 6177 (1995).
- [20] Z. Xiong, H. Chen and L. Lu, Nucl. Phys. B **561**, 3 (1999).
- [21] C. D. Carone and Y. Su, Phys. Lett. B **344**, 2015 (1995).
- [22] Y. Su, Phys. Rev. D **56**, 335 (1997).

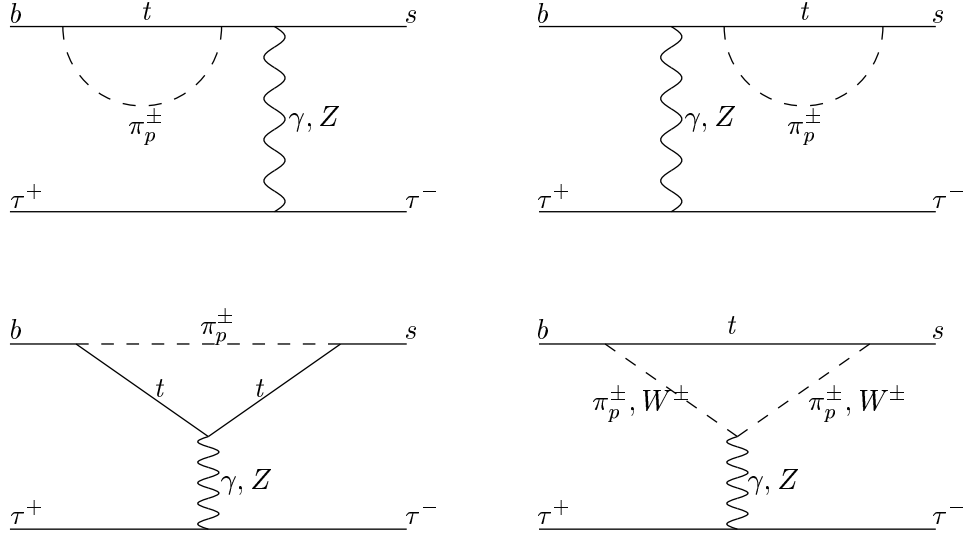


FIG. 1. Feynman diagrams for the charged scalar contributions in technicolor with scalars.

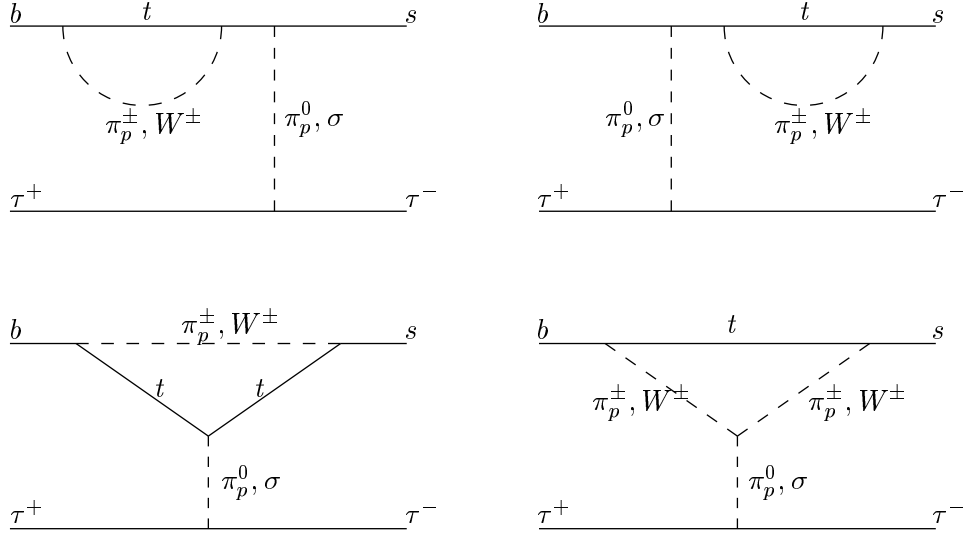


FIG. 2. Feynman diagrams for the additional contributions from the neutral scalars in technicolor with scalars.

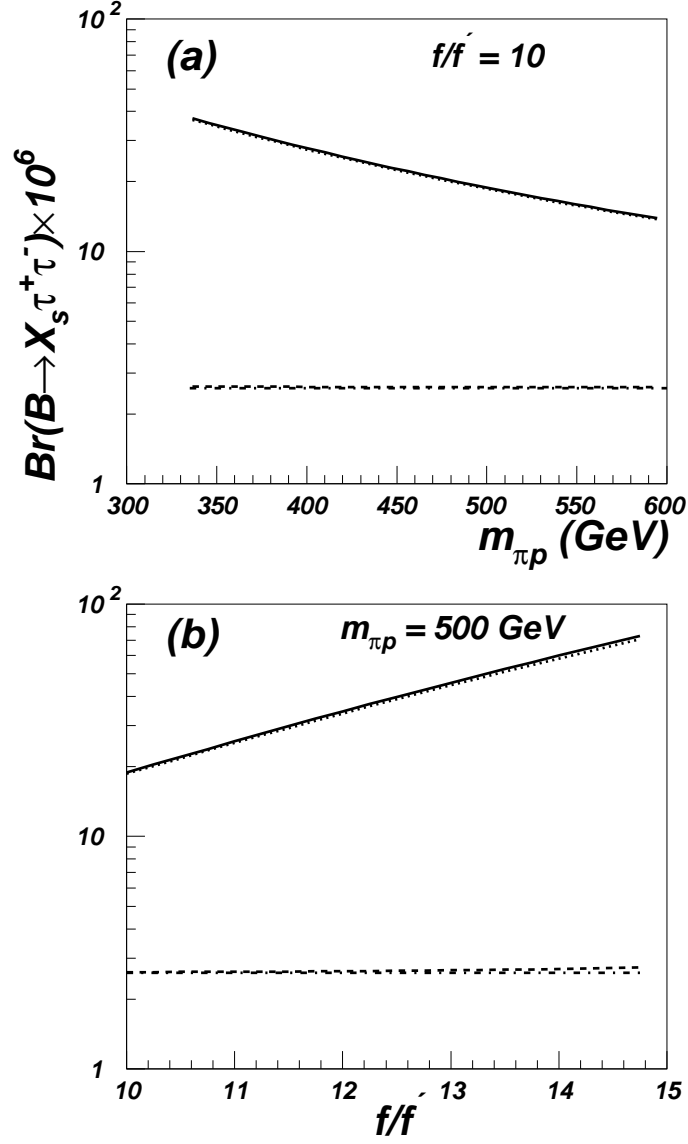


FIG. 3. Branching ratio of  $B \rightarrow X_s \tau^+ \tau^-$  versus  $m_{\pi p}$  for  $f/f' = 10$  (a), and versus  $f/f'$  for  $m_{\pi p} = 500$  GeV (b). The dot-dashed line stands for the SM prediction. The dotted (dashed) lines denote the new physics contributions from  $\gamma$ ,  $Z$  exchange (neutral scalar exchange) diagrams shown in Fig. 1 (Fig. 2). The solid one is the total values.

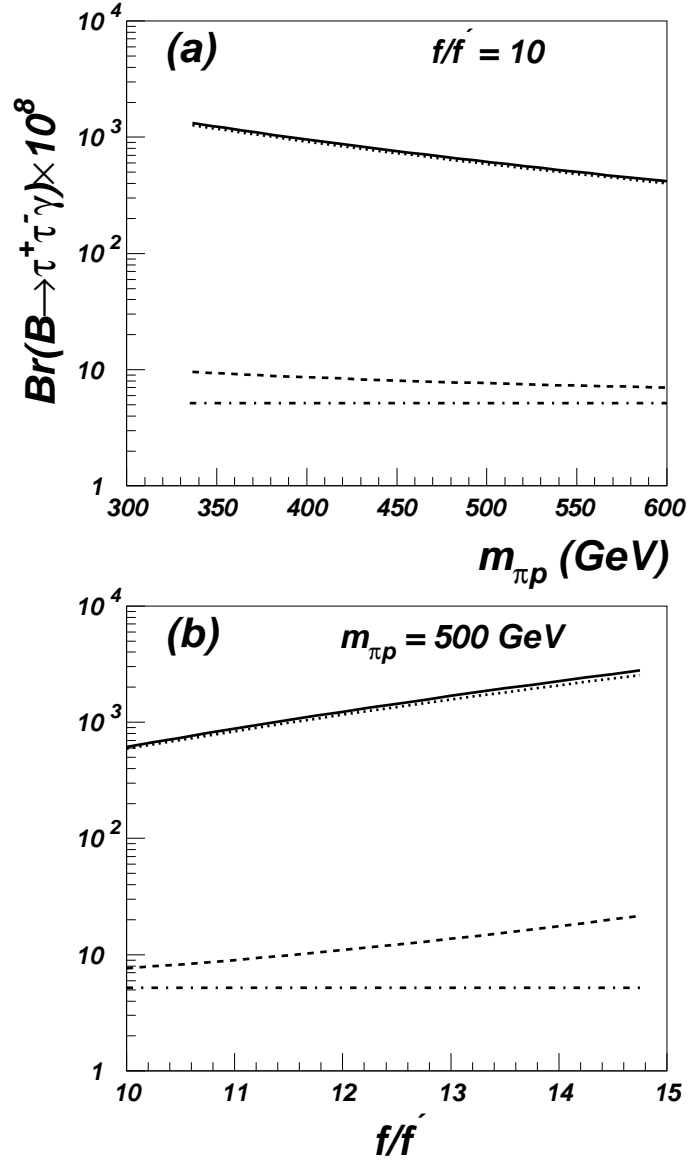


FIG. 4. The same as Fig. 3, but for  $B_s \rightarrow \tau^+ \tau^- \gamma$ .

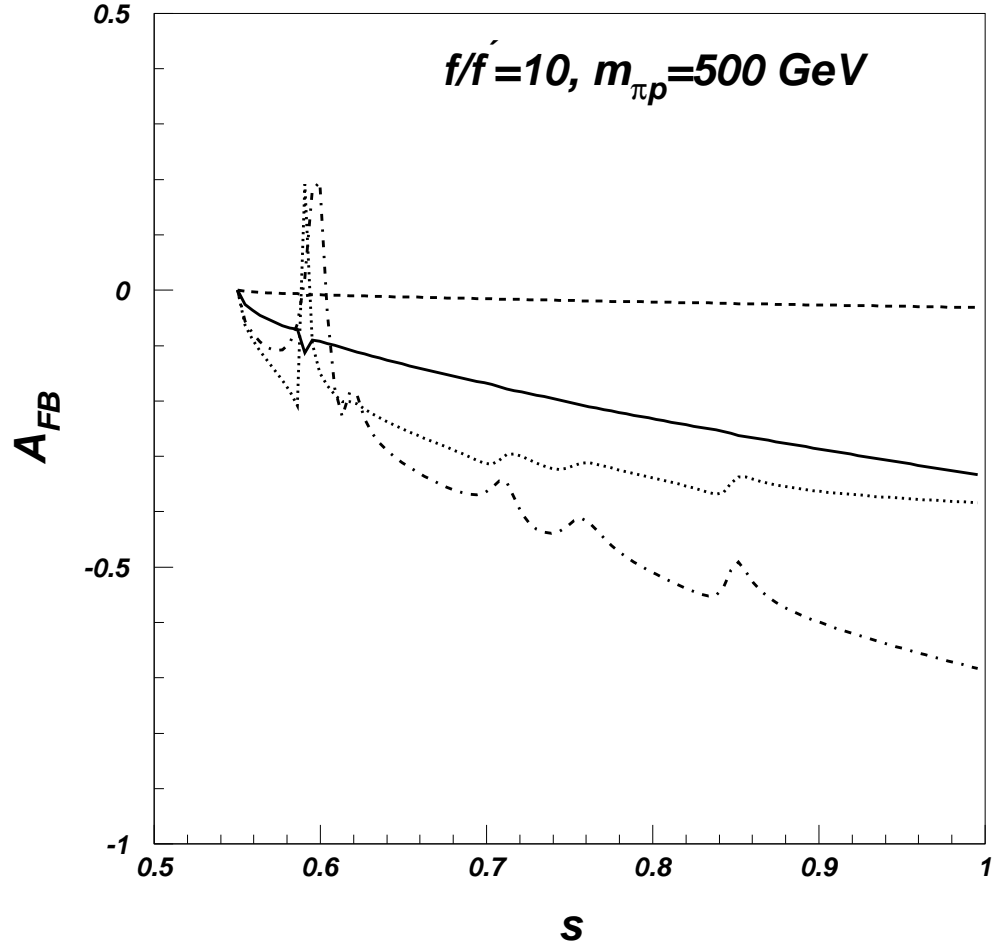


FIG. 5. The same as Fig. 3, but for the forward-backward asymmetry of  $B \rightarrow X_s \tau^+ \tau^-$  versus the scaled invariant dilepton mass squared  $s$  with  $f/f' = 10$  and  $m_{\pi p} = 500 \text{ GeV}$ .

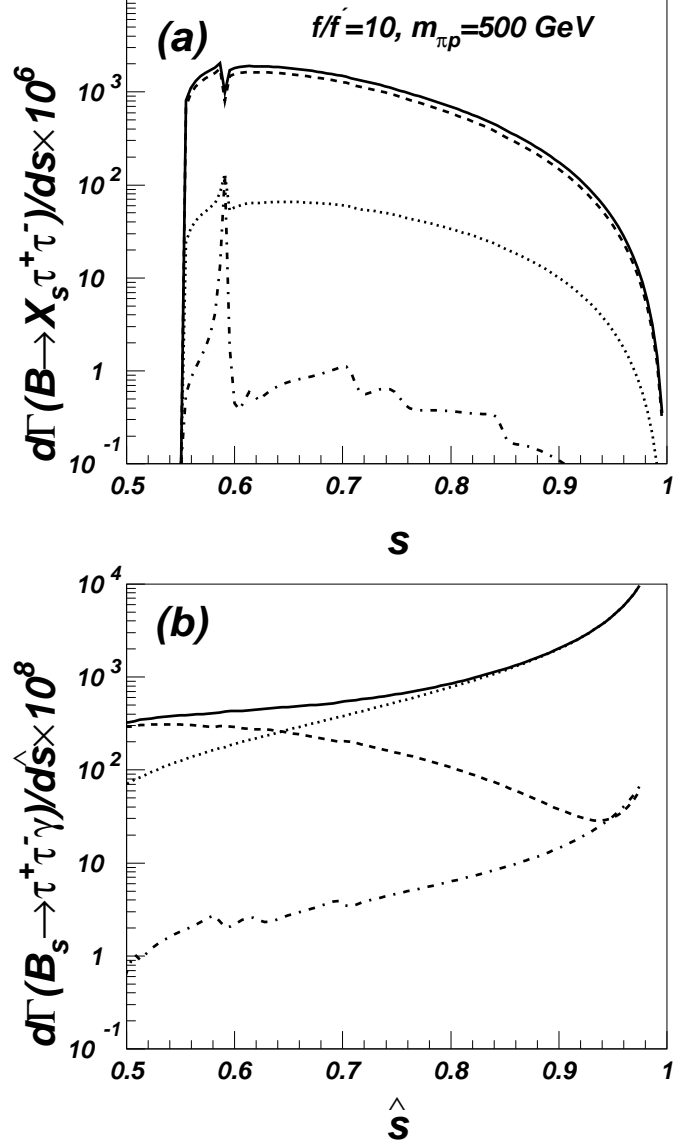


FIG. 6. The same as Fig. 3, but for the differential branching ratios of  $B \rightarrow X_s \tau^+ \tau^-$  and  $B_s \rightarrow \tau^+ \tau^- \gamma$  versus the scaled invariant dilepton mass squared with  $f/f' = 10$  and  $m_{\pi p} = 500$  GeV.